Journal of
Plankton Research

academic.oup.com/plankt

J. Plankton Res. (2020) 42(1): 87–101. First published online January 25, 2020 doi:10.1093/plankt/fbz076

ORIGINAL ARTICLE

Fecundity and early life of the deep-water jellyfish *Periphylla periphylla*

ULF BÅMSTEDT[1,*], ILKA SÖTJE[2], HENRY TIEMANN[2] AND MONICA BENTE MARTINUSSEN[3]

[1]UMEÅ MARINE SCIENCES CENTRE, UMEÅ UNIVERSITY, NORRBYN 557, SE-905 71 HÖRNEFORS, SWEDEN, [2]UNIVERSITÄT HAMBURG, INSTITUTE OF ZOOLOGY, MARTIN-LUTHER-KING-PLATZ 3, 20146 HAMBURG, GERMANY, AND [3]INSTITUTE OF MARINE RESEARCH, NORDNESGATEN 50, N-5005 BERGEN, NORWAY

*CORRESPONDING AUTHOR: ulf.bamstedt@umu.se

Received April 4, 2019; editorial decision December 20, 2019; accepted December 20, 2019

Corresponding editor: Marja Koski

Comparisons over 6 years of three Norwegian fjord populations of the deep-water scyphomedusa *Periphylla periphylla* are presented. A minor part of the population in Lurefjord is migrating to the surface during night, which benefits mating encounters by increasing abundance per unit volume and decreasing the distance between individuals. Simulations using a typical water-column density profile and Stoke's law show that fertilized eggs released in the surface quickly reach a depth where light is insufficient for visual predators. Consequently, the distribution of the smallest juveniles was strongly skewed towards higher depths in all three fjords studied. Mature females in Sognefjord were 4–5 times less abundant than in Lurefjord and Halsafjord, but due to a larger size and strong exponential relationship between size and number of mature oocytes, the potential recruitment rate as recruits m^{-2} $year^{-1}$ was not much different from the other two fjords. Nevertheless, the observed number of small (<1 cm) juveniles was 18–31 times higher in Sognefjord than in the other two fjords, and it is assumed that the deeper habitat (up to 1300 m) compared to the other fjords (up to 440 and 530 m) is a superior habitat for the early development of *P. periphylla*.

KEYWORDS: jellyfish reproduction; jellyfish blooms; jellyfish fecundity; *Periphylla* recruitment; fjord ecology

INTRODUCTION

The coronate holopelagic scyphomedusa *Periphylla periphylla* has a multi-year life span (Jarms *et al*. 1999) and a worldwide distribution, recorded from northern polar (Dalpadado *et al*. 1998) to southern polar waters (Pages *et al*. 1996), and from Atlantic (Lucas and Reed 2010) as well as from Pacific waters (Osborn *et al*. 2007). Early reports on mass occurrence in Norwegian fjords have been published for Sognefjord (Broch 1913), Halsafjord (Sneli 1984) and Lurefjord (Fosså 1992)—the latter also including local information from fishermen of mass occurrence since the early 1970s. Scientific documentations of mass occurrences also include Vefsnfjord (66°N, Bozman *et al*. 2017) and Trondheimsfjord (63–64°N,

available online at academic.oup.com/plankt

Tiller *et al*. 2017, originally reported in two unpublished master theses). Recent findings by Geoffroy *et al*. (2018) increase the northerly distribution to above 80°N in Svalbard waters.

Although media reports on *P. periphylla* may indicate increased occurrence of the species along the Norwegian coastline (Tiller *et al*. 2017), this is an open question, since it might only reflect increased public interest. The hypothesis of Tiller *et al*. (2017) of a northward spreading in Norwegian fjords, due to climate warming is not logic, since the species thrives in oceanic cold deep-sea environments (Larson 1986; Larson *et al*. 1991). Mass occurrence of *P. periphylla* causes problems for the local fisheries by clogging nets and trawls and also by keeping fish away from such fjords (Tiller *et al*. 2015). The behaviour of the species includes a diel vertical migration, first described by Youngbluth and Båmstedt (2001) from Remotely operated underwater vehicle (ROV)-based video profiles and later described for individual medusa by (Klevjer *et al*. 2009; Kaartvedt *et al*. 2015), based on records from a submersed echo-sounder. Dupont *et al*. (2009) used a light-sensitivity model to show that the main part of the population in Lurefjord was adapted to a defined range in ambient irradiance level, which governed a diurnal vertical migration. Bozman *et al*. (2017) found that a major part of the big individuals remained in the ambient irradiance range between 5×10^{-5} and 1×10^{-7} μmol quanta m^{-2} s^{-1}, thereby causing a driving force for diurnal vertical migration. A long-term study with submersed echo-sounder (Kaartvedt *et al*. 2011) revealed four different behavioural groups, ranging from no vertical migration to vertical migration both day and night.

The optical environment obviously governs the vertical distribution of organisms but has probably also a profound importance for the balance between visual (e.g. fish) and tactile (e.g. jellyfish) predators in marine habitats (Eiane *et al*. 1999, Aksnes *et al*. 2009). Advective exchange of water between the fjord and the open sea is another crucial factor with strong potential impact on planktonic fjord populations. Sørnes *et al*. (2007) presented a model for explaining *P. periphylla* retention in three Norwegian fjords, based on vertical distribution and advection and with light attenuation as a governing factor for the vertical distribution. Although the model gives a logic explanation for why the three fjords can have a sustainable population of *P. periphylla*, it does not explain the mechanism behind the strong population differences in abundance of small individuals between the three studied fjords (see Sørnes *et al*. 2007). This is mainly due to a lack of basic biological information. Our main aim in this study was therefore to test if any differences in fecundity, related to size distribution of adult females in Lurefjord, Halsafjord and Sognefjord, could explain differences in abundance and size structure between the fjords. We also present field data and simulation results that show the benefit of nighttime surface aggregation and reproduction of mature medusae and fast sinking to deep water of released eggs.

MATERIAL AND METHOD

Material for this study was collected from three fjords on the western coast of Norway (Fig. 1). Lurefjord is around 20 km in length with a narrow and shallow, 20-m-deep, sill towards the open sea and the deepest part being 440 m. Sognefjord has a length of 205 km with the deepest part of the sill towards the open sea at ca 165 m and the deepest basin reaching more than 1300-m depth. Halsafjord is a side fjord of Vinjefjord, which has several other side fjords. It has no true sill, but the exchange between Halsafjord and the open sea is restricted by the shallowest area outside the fjord arm, which is 130 m deep. Halsafjord is ca. 45 km in length and with the deepest part going down to ca. 530 m.

Population structure

Quantitative sampling was made with a modified Isaac-Kid net (MIK net) with 2-m opening diameter, 500-μm mesh size and ca. 12-m length, and with a large plastic bag as a non-filtering cod-end. The net with a heavy weight in the end was slowly hauled (ca. 0.5 m s^{-1}) vertically from close to the bottom to the surface. The coronal diameter (diameter over the coronal furrow; see Jarms *et al*. 1999) of all collected individuals >1 cm was measured, whereas all individuals <1-cm diameter were only counted. Our presented MIK-net data are from 15 cruises during 6 years, 2000–2005 (Table I), and taken from the deepest part of the basin in each fjord. For Lurefjord, the estimate of average abundance was based on 1181 individuals from 51 net hauls collected during 15 cruises, for Halsafjord 352 individuals from 15 net hauls during 5 cruises and for Sognefjord, it was based on 39 individuals from 13 net hauls during 8 cruises (Table I). In order to determine the sex ratio, we used only net hauls where sex was determined on individuals of mature size (>5 cm coronal diameter; Tiemann *et al*. 2009). This reduced the number to 688 individuals in Lurefjord and 262 individuals in Halsafjord. We estimated the abundance of mature female by using the abundance of all individuals ≥5 cm diameter multiplied with the female:male ratio. Sex was not determined for individuals in Sognefjord (Table I). We, therefore, used the average sex ratio from the two other fjords to calculate female abundance and potential recruitment rate in Sognefjord. In order to

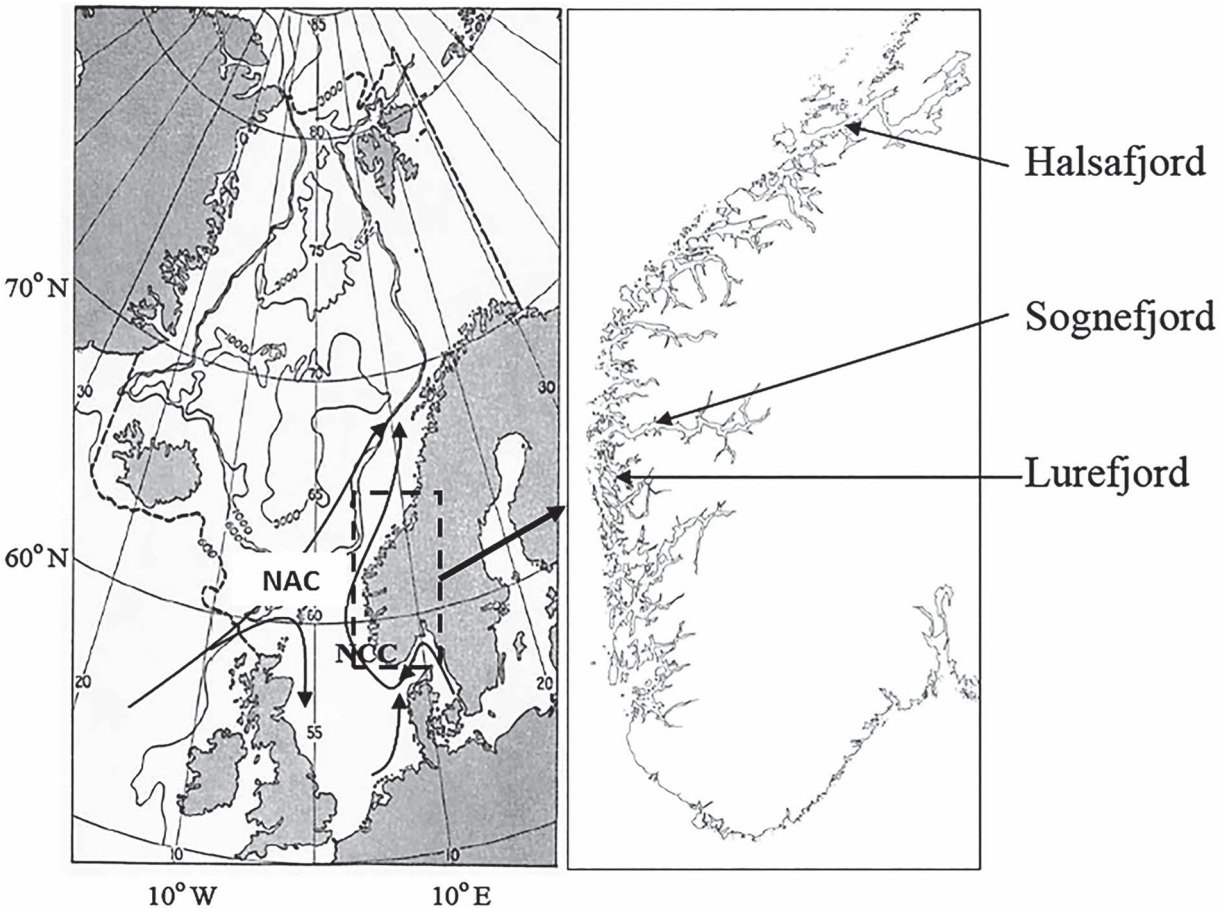

Fig. 1. Geographic location of the three Norwegian fjords in the study. NAC = Norwegian Atlantic Current; NCC = Norwegian Coastal Current.

describe the vertical distribution of juvenile individuals <1 cm in coronal diameter, we used a Hydrobios Midi Multinet (https://www.hydrobios.de/) with an opening size of 0.25 m^2 and with five nets of 300-µm mesh size and opening and closing of each net controlled from the deck. We present one example, taken between 22 and 25 June 2002 during the light part of the day.

Surface occurrence in Lurefjord

Counting *of P. periphylla* during night was made in spring 2002, 2004 and 2005. The research ship moved with an average speed of 135 m min^{-1} (02 April), 125 m min^{-1} (04 April) and 178 m min^{-1} (05 May) throughout the length of the fjord and all individuals that were detected within a floodlight beam with a width on the surface of 5 m were recorded. In 2002 and 2004, the cumulative number of medusae counted over intervals of 1 minute were recorded, whereas in 2005, we counted medusa over 5 minutes intervals and made separate recordings on the starboard and port side of the ship. By knowing the total distance, total time and beam width on the surface, abundance and geographic position could be calculated.

Histology

Specimens for oocyte examination were collected with an MIK-net in May and November 2005. The coronal diameter was measured, and gonadal tissue was immediately preserved in 4% paraformaldehyde/seawater solution. The tissue was later dehydrated and embedded in paraplast. Sections of 5–10-µm thickness were stained with nuclear fast red aluminium sulphate and light green yellowish (Tiemann and Jarms 2010). Seven cut-section series of four different mature female gonadal tissues were used for microscopic examination of oocyte morphology. Due to shrinkage during preparation and storage, a correction factor of 25% was used to estimate morphometric sizes on fresh material (Romeis 1989, Holst and Laakmann 2014). When defining the oocyte maturity state of different oocytes, we solely used yolk and nucleus structure (see Table I). The corrected minimum size for fresh

Table I: Overview of number of measured P. periphylla with a size of ≥5-cm coronal diameter, collected during 15 research cruises between March 2000 and May 2005 and used for the estimate of average abundance and sex ratio.

Cruise time	Lurefjord	Halsafjord	Sognefjord
March 2000	2:20 (13)	No sample	No sample
August 2000	3:13	No sample	No sample
October 2000	4:23	No sample	1:2
December 2000	6:22	1:82	No sample
February 2001	5:118	No sample	1:2
October 2001	3:177	No sample	4:7
March 2002	3:54	No sample	No sample
April 2002	4:84	No sample	No sample
June 2002	4:65 (5)	4:81 (39)	1:1
March 2003	4:205 (132)	4:79 (40)	3:16
October 2003	4:176 (117)	3:60 (60)	1:1
January 2004	2:58 (24)	No sample	No sample
April 2004	2:29 (29)	No sample	1:2
October 2004	2:89 (62)	No sample	1:8
May 2005	3:48 (31)	3:50 (37)	No sample

First number is the number of net hauls, number after colon is the number of sampled individuals and the number in parenthesis gives the number of individuals that were defined to sex, which was the basis for the numeric relationship between females and males.

mature oocytes, given in Table I, was then used when defining the number of mature oocytes in unpreserved gonads.

A total of 53 females in the size range 4.0–14.0-cm coronal diameter were collected from the three fjords for enumeration of mature oocytes, 49 from Lurefjord, 2 from Halsafjord and 2 from Sognefjord. Counting of fresh mature oocytes was performed directly after collection, using a stereo microscope. A scatter plot of number of mature oocytes versus female coronal diameter was made and the best-fit regression equation calculated, thereby excluding three females (4.0-, 6.0- and 6.5-cm coronal diameter) with no mature oocytes. We also included a single 16.0-cm diameter female collected from Osterfjord, ca. 15 km south of Lurefjord and calculated the best fit exponential regression equation both with and without the female from Osterfjord.

Maximum size of oocytes

In a separate study, females in the size from 6- to 14-cm coronal diameter were collected with a Harstad trawl in the period April—June 2002. Measurements of maximum oocyte size were done on 120 females from Lurefjord and 129 females from Halsafjord Care was taken to cover the whole size spectrum of females with gonads visible by the naked eye. A digital camera was used to take macro-photos of parts of the gonads containing the biggest oocytes. The diameter of the biggest oocytes was calculated by using the software Scion Image (Scion Corporation, USA) with a micro-ruler as a standard and scatter plots of maximum oocyte diameter versus female coronal diameter were made.

Estimating female fecundity and potential recruitment rate

The relationship between female size and number of mature oocytes was used on all individuals that were identified as mature females, and the sum, divided by the number of females included, gave the average number of mature oocytes per female ($N_{oocytes}$), which will be a relative measure of fecundity. These results were then used to simulate the fecundity, expressed as spawned eggs female^{-1} year^{-1}, i.e.

$$\text{Fecundity} = \mathcal{N}_{\text{oocytes}} \times 12/\text{T}$$

where T is the turnover time (months) for newly matured oocytes to being released. The constant T is unknown, and we simulated fecundity with T set to 1, 3, 6 and 12 months. By also knowing the average abundance of mature females in the three fjords ($\mathcal{N}_{\text{females}}$), these simulations also generated potential recruitment rates, i.e.

$$\text{Potential recruitment rate} = \text{Fecundity} \times \mathcal{N}_{\text{females}}$$

Both equations can be expressed as a simple inverse relationship:

$$\mathcal{Y}_{\text{i}} = \mathcal{Y}_1 \times 12/\text{T}$$

where Y_i and Y_1 is the fecundity or recruitment rate with turnover time i months, respectively, 1 month.

Factors governing the life cycle

Tiemann *et al*. (2009) suggested that the occurrence of mature *P. periphylla* in the surface water represented a

mating behaviour. In order to illustrate the increase in encounter probability by migration to the surface, we calculated both the change in abundance per volume of water and the average distance between individuals in an even distribution when gradually decreasing the vertical distribution to the uppermost surface water. Information from Jarms *et al*. (2002) on vertical distribution of planktonic eggs in Lurefjord suggested that these are pelagic and remain far below the surface water. We therefore simulated a scenario where eggs are released in the surface water, but have a density corresponding to the depth where they have been observed by Jarms *et al*. (2002). We used Stoke's law on sinking velocity of spherical objects in fluids that in a simplified way (see Mann and Lazier 1998) can be expressed as:

$$V_i = \frac{2}{9} g \times r^2 \left(\rho' - \rho_i\right) / \left(\rho_i \times v\right)$$

where V_i is the sinking velocity in m s^{-1} at depth i, g is the gravity acceleration constant, 9.81 m s^{-2}, r is the radius (m) of the object, ρ' *and* ρ_i is the specific density (g cm^{-3}) of the object and the surrounding water at depth i, respectively, and v is the kinematic viscosity of the water, which can be set to 10^{-6} m^2 s^{-1} for waters within a natural range in temperature. Time in seconds $T(D_N)$ to reach a given depth (D_N) can then be calculated as:

$$T\left(D_N\right) = \sum_{i=0}^{N} \left[\mathrm{D\,(i)} - D\left(i-1\right)\right] / V_i$$

As an index of changed predation pressure in Lurefjord from vision-dependent predators, such as fish, we measured the absolute irradiance both at the wavelength penetrating deepest (567.8 nm), and for the whole visible spectrum (400–700 nm) down to 43 m on mid-day, 13 May 2005, using an Ocean Optics radiometer (Ocean Optics, Winter Park, Florida, USA), connected to a fibre-optic cable. We calculated the light attenuation for both series by fitting exponential regression equations to the data.

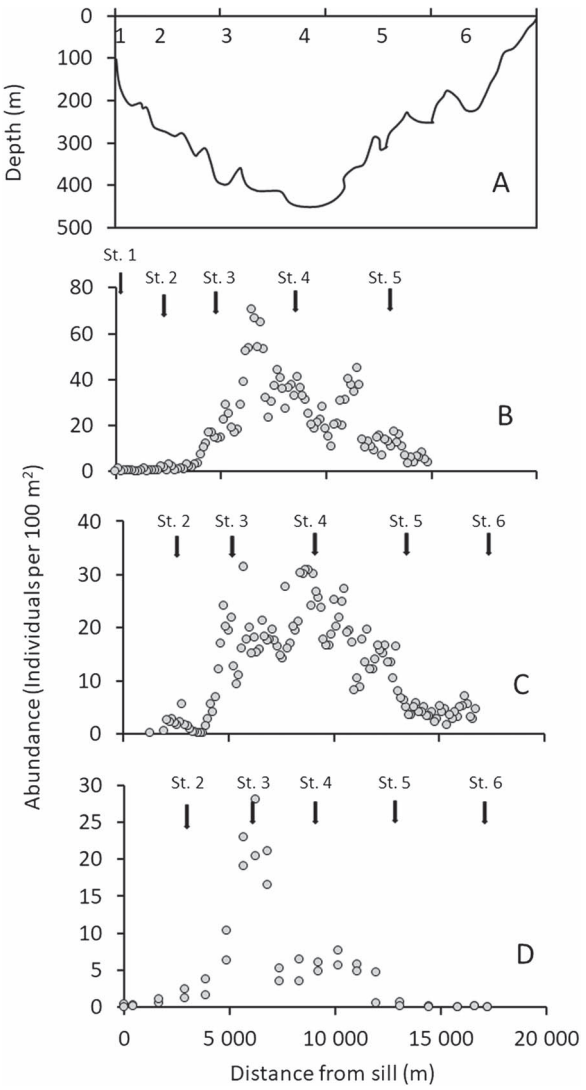

Fig. 2. Night abundance in the surface of *P. periphylla* in Lurefjord along a transect from the outer to the inner part of the fjord. A. Bottom topography. B. April 2002, C. April 2004, D. May 2005. Positions of stations for quantitative sampling of the whole water column are indicated in all graphs.

RESULTS

Surface aggregation

Night-time longitudinal transects through Lurefjord with quantitative counting of surface occurrence showed roughly the same results for three different years (Fig. 2). Highest abundance was observed at the deeper part of the fjord, where peak abundance ranged between 28 and 70 individuals 100 m^{-2} (Fig. 2). The abundance in the whole water column was usually two orders of magnitude higher, reaching a peak abundance of, respectively, over 4000, over 2000 and almost 800 individuals 100 m^{-2} in the three surveys, and a peak biomass of more than 2-kg wet weight m^{-2} in 2002 and 2004 and almost 1 kg m^{-2} in 2005 (Table II).

Fig. 3A illustrates the increase in encounter probability between individuals as a function of vertical distribution and with four different water columns as examples. Since the aggregation is doubled with each reduction to half depth, the strongest effect is in the uppermost part of the water column. For a population distributed in 1000 m, the aggregation is increase by a factor of 2 when reducing the distribution to 500 m, and by a factor of 10 by

Table II: P. periphylla: Morphological features of oocytes in the female gonad, based on 5–10-µm semi-sections.

Oocyte stages	Description	Diameter preserved material [µm]	Approximate diameter fresh material [µm]
Mature	**Yolk**: differentially structured, marginal layer containing small granules (d = 3 µm), inner sphere filled with yolk granules (d > 10 µm). **Nucleus**: located at the oocyte margin (d = 200–240 µm), without basophilic or acidophilic reaction, with distinctive nucleolus	874.4 ± 118.4 µm Min 710 µm Max 1020 µm N = 9	1000–1200 µm
Immature largest	**Yolk**: uniform (d = 4 µm). Oocyte marginal layer free off yolk granules. **Nucleus**: located in the centre of oocyte (d = 130 µm), with weak basophilic reaction, with distinctive nucleolus	339.2 ± 33.0 µm Min 300 µm Max 390 µm N = 6	400–530 µm
Immature second largest	**Yolk**: uniform (d = 4 µm). **Nucleus**: located in the centre of oocyte (d = 100 µm), with strong basophilic reaction, with distinctive nucleolus	258. 0 ± 8.9 µm Min 250 µm Max 270 µm N = 5	330–360 µm

Average oocyte diameter ± 1 standard deviation given. d = diameter. Sizes of fresh material calculated by using a shrinking factor of 25% (Romeis 1989; Holst and Laakmann 2014).

Table III: Abundance, biomass and size (mean +/− standard deviation) of P. periphylla in Lurefjord in spring during 3 years.

Sample	Water column N/100 m^2	kg/m^2	Mean CD	N	Surface N/100 m^2	% in surface
Apr-02						
Stn. 1	414	0.14	3.12 ± 2.06	13	0	0
Stn. 2	3694	0.87	2.07 ± 1.82	116	0	0
Stn. 3	4331	1.93	3.02 ± 2.37	136	14.2	0.33
Stn. 4	2133	2.26	5.11 ± 2.90	67	40.6	1.90
Stn. 5	828	0.77	4.60 ± 2.83	26	15.7	1.90
Stn. 6	-	-	-	-	-	-
Apr-04						
Stn. 1	0	0	-	0	-	-
Stn. 2	287	0	3.58 ± 2.19	9	0.5	0.17
Stn. 3	1529	1.17	4.13 ± 2.47	48	21.8	1.43
Stn. 4	2357	2.06	4.53 ± 2.39	74	20.2	0.86
Stn. 5	319	0.02	1.65 ± 0.82	10	13.4	4.20
Stn. 6	32	0.08	8.00	1	4.6	14.4
May-05						
Stn. 1	64	0.06	5.45 ± 0.64	2	0.18	0.28
Stn. 2	796	0.95	5.78 ± 1.75	25	0.78	0.10
Stn. 3	732	0.71	5.31 ± 1.90	23	8.31	1.14
Stn. 4	541	0.89	6.44 ± 2.33	17	4.95	0.91
Stn. 5	287	0.34	5.57 ± 2.06	9	0.43	0.15
Stn. 6	0	0	-	0	0.12	-

"Water column" means abundance based on quantitative vertical sampling from bottom to surface with an MIK net and "surface" means night-time counting of medusae occurring in the surface along a transect throughout the fjord. CD is the coronal diameter (cm). N is the number of medusae collected/observed and—denotes no data

reducing to 100 m, whereas distribution in the surface would increase the aggregation by 10 000 times (Fig. 3A). Average distance to a neighbour would be almost 22 times higher when distributed in a 1000-m water column compared to an aggregation in the surface, and for 500, 100 and 20-m dispersal, neighbour distance would be 17, 10 and 6, respectively, times higher than when aggregating in the surface (Fig. 3B).

Size distribution and fecundity

The numeric relationship between females and males of a size where sex could be determined by the naked eye (≥5 cm coronal diameter) was skewed towards females (Fig. 4A and B), which represented 64% in the population in Lurefjord and 60% in Halsafjord. The very limited catch of mature individuals by MIK net in Sognefjord indicated a considerably higher size of mature individuals

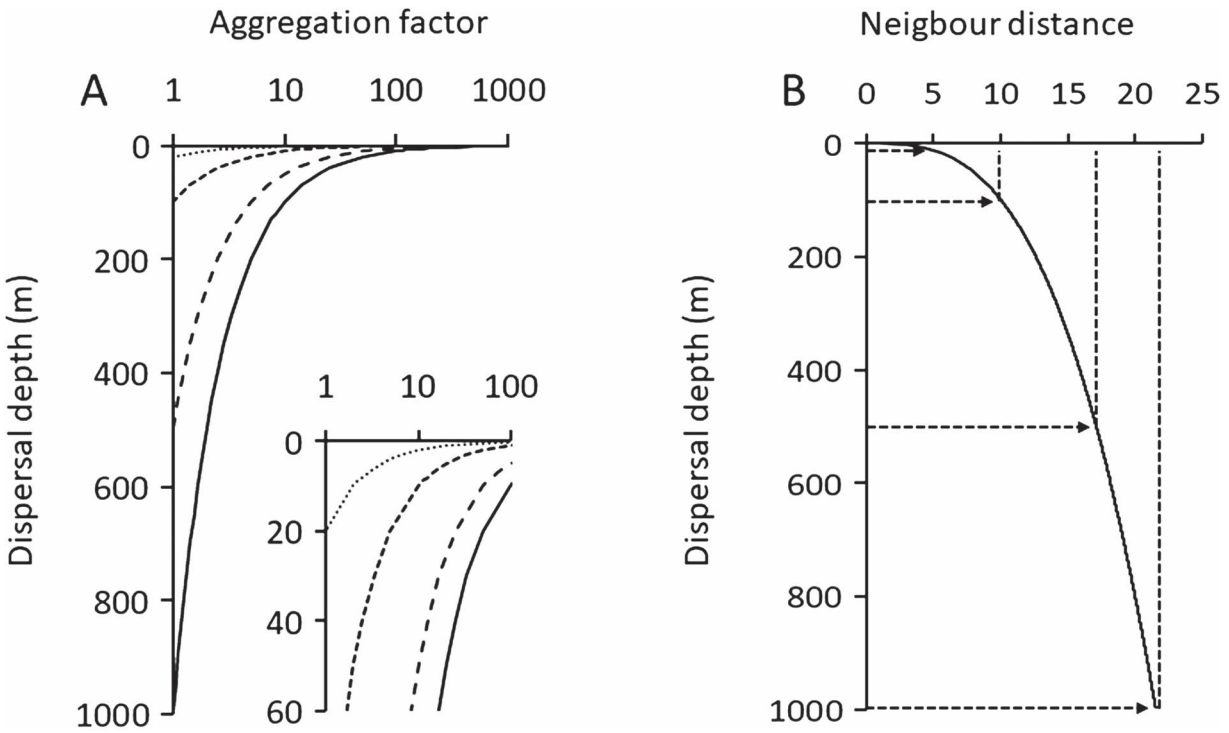

Fig. 3. A. Aggregation factor, expressed as increase in abundance per unit water volume, as a function of dispersal depth, of a population with uniform distribution and a fixed abundance per m^2. Curves in A represent populations dispersed in 1000, 500, 100 and 20 m, respectively, and the inserted graph is an expansion of part of the graph for clarity. B. Relationship between relative distance to a neighbour and dispersion depth of a population as in A. The dotted lines in B indicate the depths 20, 100, 500 and 1000 m. Dispersal in the surface only is calculated as dispersal in the uppermost 0.1 m of water column.

than in the two other fjords (Fig. 4C). Average size for mature individuals was 7.6 cm for females and 8.1 cm for males in Lurefjord, 8.8 cm for females and 9.3 cm for males in Halsafjord, and the average size of mature individuals in Sognefjord, not determined to sex, was 11.5-cm coronal diameter. The average number of females of mature size per 100 m^2 was similar in Lurefjord and Halsafjord (444 and 476, respectively), whereas females in Sognefjord were less abundant, with 96 females per 100 m^2 (Fig. 4).

The variation in abundance between cruises was considerable, with a range from 1.2 to 19.6 females m^{-2} in Lurefjord and from 5.1 to 21.3 females m^{-2} in Halsafjord (Fig. 5A). The average size of females of mature size was less variable between cruises, with a range from 6.3- to 9.7-cm diameter for the population in Lurefjord and 7.6 to 10.0 cm for Halsafjord (Fig. 5B).

The number of mature oocytes in the female gonads was strongly related to female size (Fig. 6) and around 80% of this relationship was explained by the exponential regression line. Measurements of maximum oocyte size of 120 females from Lurefjord indicated that oocytes reached the proposed maturity size of 1 mm (cf. Table II) at around 6-cm coronal diameter Fig. 7), but that also a minor part of the females over the whole size range lacked mature oocytes (Fig.7). We interpret this as representing females that had recently released all their mature oocytes. Females from Halsafjord carried mature oocytes from around 7-cm coronal diameter and always carried oocytes of mature size when exceeding a size of 9–10 cm coronal diameter.

Since we do not know the reproduction rate, we can simulate the fecundity and potential recruitment rate by using the original relationship given in Fig. 5 and different turnover times of mature oocytes. Fig. 8 shows the results for the three fjord populations with simulated turnover times of 1–12 months. With 1-month turnover time the average female fecundity in the Sognefjord population would be over 8000 pelagic eggs per year, whereas a turnover time of 1 year would reduce this to roughly 700 (Fig. 8A). The results for the two other fjords would be roughly700 and 60 (Lurefjord) and 1400 and 120 (Halsafjord). The potential recruitment rate in the three fjords would be highest in Sognefjord, with roughly 0.8 million recruits 100 m^{-2} $year^{-1}$, using a turnover time of 1 month and with 667 000 (Halsafjord) and 316 000 (Lurefjord) recruits 100 m^{-2} $year^{-1}$ for the two other fjords. A turnover time of 1 year would reduce these

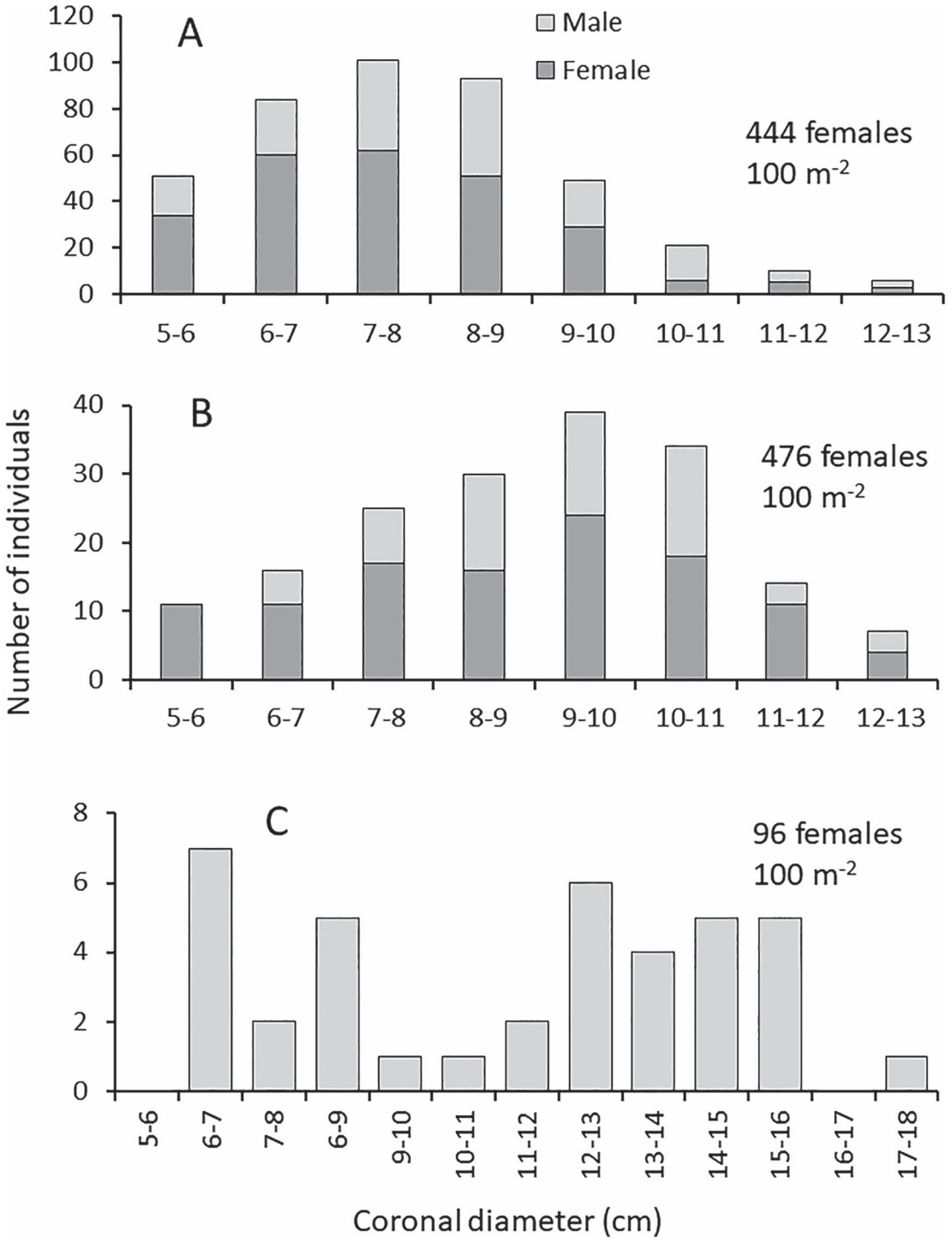

Fig. 4. Size distribution of mature female and male (>5 cm coronal diameter) *P. periphylla* in Lurefjord (A), Halsafjord (B) and Sognefjord (C). For Lurefjord, the data are from 8 cruises between March 2000 an May 2005; for Halsafjord, the data are from four cruises between June 2002 and May 2005, and for Sognefjord the data are from eight cruises between October 2000 and October 2004, without information on sex. Average abundance of females per 100 m^2, based on all samples (see Table I) is given in each graph.

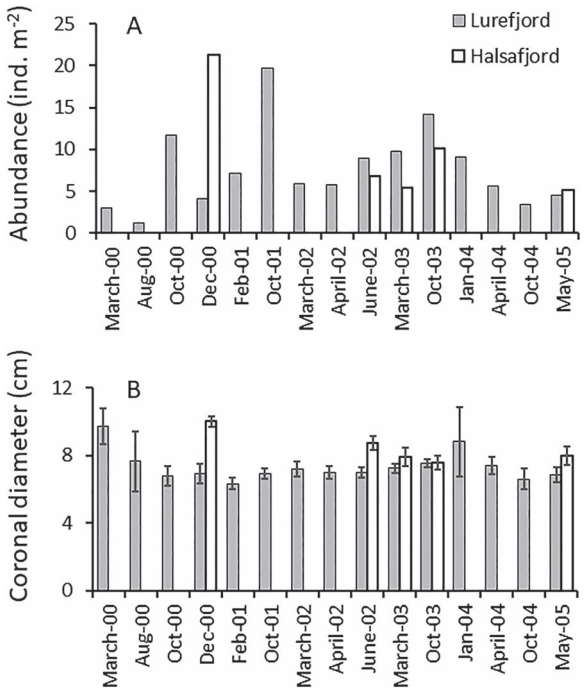

Fig. 5. A. Average abundance (A) and size (B) of *P. periphylla* of adult size (≥5 cm diameter) in the deepest part of Lurefjord and Halsafjord. Size is given as coronal diameter +/− 95% confidence interval. Results based on total data from net hauls as shown in Table I.

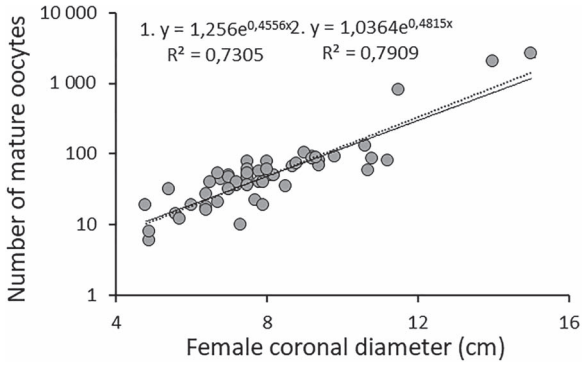

Fig. 6. Relationship between female size and number of mature oocytes of *P. periphylla* from the three studied fjords. The triangle represents a single female from Osterfjord, excluded in equation 1 (solid line) and included in equation 2 (broken line).

numbers to 12 times less, as shown by the displayed equation in the graph (Fig. 8B).

Juvenile habitat

Eggs and young motionless stages are pelagic, and by necessity also neutrally buoyant in their habitat, and probably also remain in the deeper part of the water column (Jarms *et al*. 2002). Our multi-net data from

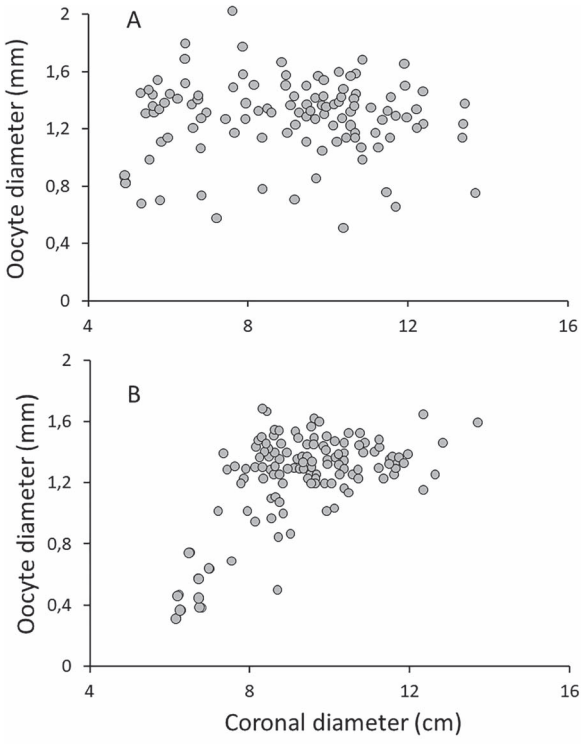

Fig. 7. Scatter plot of maximum oocyte diameter versus female size in the gonads of *P. periphylla* collected in April and June 2002 from (A) Lurefjord (120 females) and (B) Halsafjord (129 females). Each point represents one female.

Lurefjord, Halsafjord and Sognefjord on vertical distribution of juveniles <1 cm in diameter, which corresponds to developmental stages up to 11 or 12 (cf. Jarms *et al*. 2002), show that they have a vertical distribution, which is strongly skewed towards the deepest sampling depths in all three fjords (Fig. 8). Although all individuals included in the samples are not motionless, the results indicate that the very early development is spent in the deeper part of the water column. Combined with an assumed reproduction in the surface water, this means that the released eggs are sinking to a depth corresponding to their neutral buoyancy. We have, therefore, simulated how eggs released in the surface and with a density corresponding to neutral buoyancy at 300 m in Lurefjord will gradually sink to its equilibrium depth. Fig. 10A shows a typical vertical density profile in Lurefjord and Fig. 10B simulates the sinking succession over time, if egg density alone determines the sinking rate. Eggs rapidly left the euphotic zone and reached 100 m within 2 hours, 200 m in 11.6 hours and will reach neutral buoyancy depth at 290 m in ca. 41 hours (Fig. 10B). Our measurement of light penetration through the water column showed that the irradiance at 43 m had its maximum at 567.8 nm

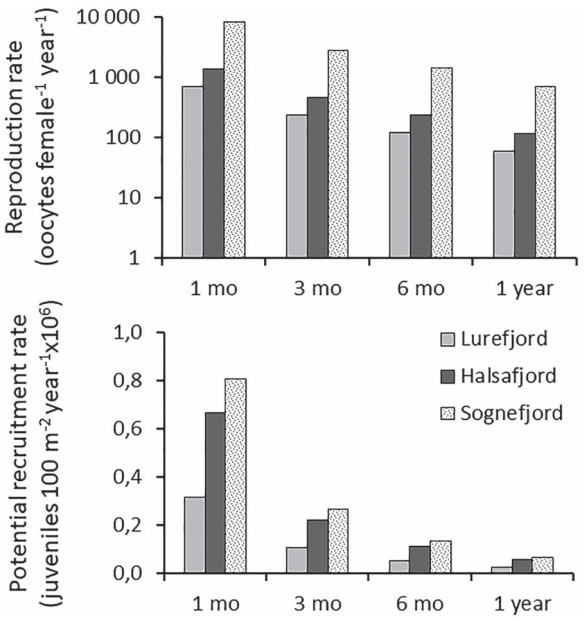

Fig. 8. (A) Simulated fecundity of an average female *P. periphylla* in the three fjords, based on average number of mature oocytes and different oocyte turnover times. (B) Simulated potential recruitment rate of juvenile *P. periphylla* in the three fjords, based on the fecundity and abundance. The equation in the graphs shows the mathematical relationship between fecundity or recruitment rate (Y) and turnover time (X).

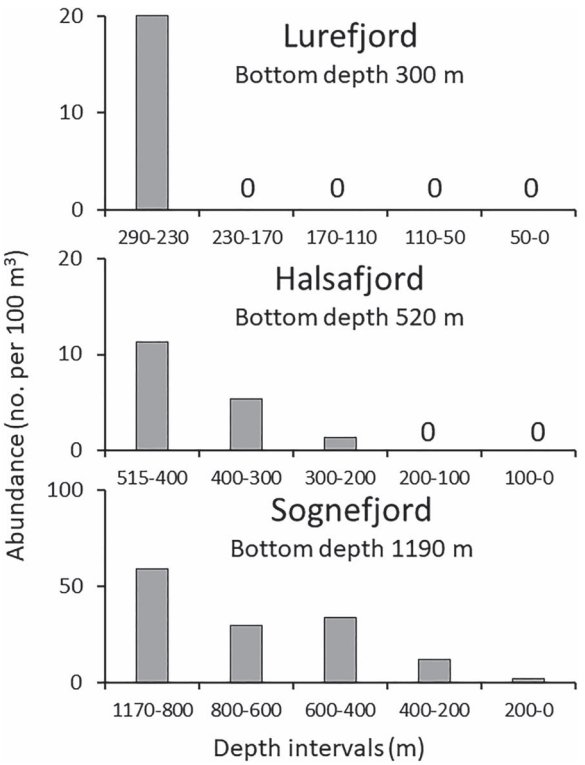

Fig. 9. Data from multinet samples showing occurrence of small (<1 cm coronal diameter) *P. periphylla* in five vertical depth intervals in Lurefjord. Halsafjord and Sognefjord. Bottom depth refers to the depth at the actual sample station. Data from June 2002.

(Fig. 9C). The attenuation coefficient for this wavelength was 0.135 m^{-1} (Fig. 8D) and the equation showed that the light had been reduced to 1% at 31 m, 0.1% at 48 m and 0.001% 83 m. The time for a released egg to reach these depths would be 8.7 minutes, 18.9 minutes, and 1.25 hours, respectively. By using results for the whole visual light spectrum in the calculations the vertical light attenuation becomes even more pronounced, described by the equation $Y = 54.997e^{(-0.169X)}$, with 1% reached at 24 m, 0.1% at 37 m and 0.01% at 65 m. Time to reach these depths would be 5.8, 11.6 and 39.0 minutes, respectively. Visual light at 200 m had then been reduced to 1.15×10^{-13}% of surface irradiance.

Discussion

Surface aggregations of large specimens of *P. periphylla* have been observed in Norwegian fjords as well as in the open ocean (Geoffroy *et al.* 2018, Tiemann *et al.* 2008, Turner and Lucas 2010, Youngbluth and Båmstedt 2001). Kaartvelt *et al.* 2015 documented apparent social behaviour in *P. periphylla*. They found that medusae are forming groups in the upper 100-m water layer and not only at the surface in Lurefjord. Very early surveys have also reported on occurrence of *P. periphylla* in surface waters (Brown 1910; Havnø 1926; Kramp 1947, 1968; Stiasny 1934). We have only observed *P. periphylla* in the surface in Lurefjord, not in Halsafjord or Sognefjord. Tiemann *et al.* (2009) showed from studies in Lurefjord that surface aggregation occurred during the night, but only with individuals of mature size, and usually as groups where both sexes were represented, occasionally with a male and female close together with entangled tentacles. They explained this as a mating behaviour. Our results from three years show the same pattern of a small part of the population migrating to the surface, and our theoretical estimate of encounter benefit (Fig. 3) shows that surface aggregation will increase the probability of two individuals to converge by several orders of magnitude, even for a population with depth distribution less than 100 m. In addition, the turbulent mixing is higher in surface water than in deep water, thereby increasing the encounter benefit further for sperms to fertilize the mature oocytes in shallow water. Okey and Elliot (1980) found that turbulent energy dissipation in the upper 50 m with a wind speed of 15 m s^{-1} was 10^{-6} W kg^{-1}, whereas it was 10^{-9} W kg^{-1} in the deep water, i.e. a difference by a factor of 10^3. Surface aggregation and mating would be even more important for open-sea

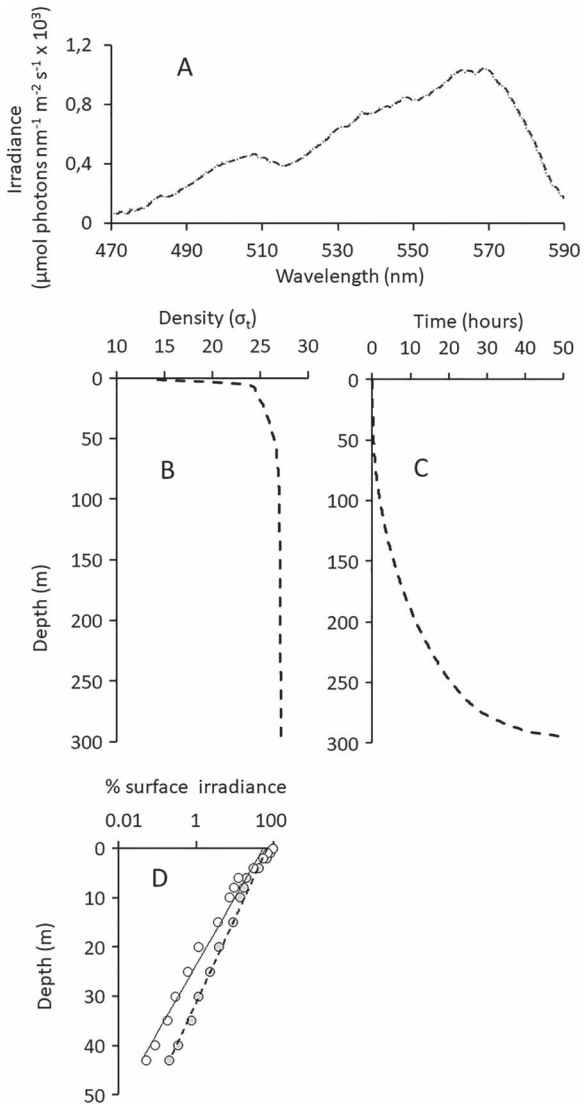

Fig. 10. A. Spectral distribution of the irradiance at 43-m depth in Lurefjord, May 2005. B. Density profile in Lurefjord in May 2005. C. Estimated sinking progress for a released egg of *P. periphylla* in the surface. D. Water-column light attenuation for visible light (400–700 nm, solid line, $R^2 = 0.980$) and 567.8 nm (broken line, $R^2 = 0.987$). Data from May 2005 and expressed as percentage of sub-surface irradiance.

populations, where the abundance is several orders of magnitude lower than in the fjord habitats.

Even though jellyfish are comparable simple organisms, a sophisticated courtship behaviour with mating is known, e.g. from several cubozoan species *Tripedalia cystophora*, *Copula* (*Carybdea*) *sivickisi* and *Alatina alata* (Werner 1973, Lewis and Long 2005, García-Rodrígues *et al*. 2018) and from hydromedusae (*Liriope tetraphylla*, Ueno and Mitsutani 1994). The medusae of *Carybdea sivickisi* use their tentacles during court-ship procedure (Lewis and Long 2005) as does *P. periphylla* during the observed surface aggregations in Lurefjord (Tiemann *et al*. 2009, Kaartvedt *et al*. 2015).

In general, spawning aggregations enable a fertilization with oocytes attached to the moutharms, within the gastric cavity or even within the ovary in various species like *Mastigias papua*, *Tripedalia cystophora*, *Tripedalia binata*, *Carybdea alata*, *Nemopilema nomurai*, *Alatina alata*, *Copula sivickisi*, *Cyanea capillata*, *Cyanea arctica*, *Aurelia aurita*, *Aurelia flavigula*, *Chrysaora hysoscella*, *Rhizostoma pulmo*, *Rhizostoma luteum* and *Cotylorhiza tuberculata* (Uchida 1926, Werner 1973, Bentlage *et al*. 2010, Toshino *et al*. 2017, Ohtsu *et al*. 2007, García-Rodríges *et al*. 2018, Widersten 1965, Hargitt and Hargitt 1910, Kikinger 1992, Kienberger *et al*. 2018). A very interesting spawning aggregating species is the coronate *Linuche unguiculata* (*Linerges mercurius*, Conklin 1908). Specimens move actively to the surface to aggregate in calm waters. They release oocytes and spermatozoids around 8 in the morning for fertilization. The zygotes sink gradually into deeper water as do the medusae after spawning.

Some species take care for their brood within or attached to the moutharms of the mother until the planula is fully developed (e.g. *Mastigias papua*, *Rhizostoma luteum*, *Cotylorhiza tuberculata*, *Aurelia aurita*, *Aurelia flavigula*, *Cyanea capillata*, *Cyanea arctica*, *Chrysaora hysoscella and Tripedalia binata*) (Uchida 1926, Hargitt & Hargitt 1910, Widersten 1965, Toshino *et al*. 2017, Kikinger 1992, Kienberger *et al*. 2018).

We know from previous studies that eggs and early juveniles probably are remaining free floating in the deeper part of the water column (Jarms *et al*. 2002). Jarms *et al*. (1999) also found planktonic eggs and small juveniles in Lurefjord throughout the year, thus indicating continuous reproduction, later confirmed by Tiemann and Jarms (2010) from histological examinations. These authors have described how the numerous oocytes of different maturity state are orientated in horizontal folds in the eight gonads of female specimens with the largest, mature oocytes located at the tip of the gonad folds. A similar gonad structure has been described for *Pelagica noctiluca*, a species also with holopelagic life cycle and continuous reproduction (Rottini Sandrini and Avian 1991).

Eggs released in the surface water would be protected from visual predation during the dark part of the day, but if remaining in the euphotic zone during daytime, their average size of 1.17 +/− 0.09 (standard deviation) mm diameter (Jarms *et al*. 2002) makes them vulnerable to visual predation. Pelagic eggs have been found at around 230-m depth in Lurefjord (Jarms *et al*. 2002) and we can therefore assume that they have neutral buoyancy around that depth in Lurefjord. Our simulation of egg sinking progress shows that eggs released in the surface

would rapidly reach depths with strongly reduced light (Fig. 8B and D). *P. periphylla* has a porphyrin pigmentation that occurs already from small size (stage 7 with a diameter of 3.3 mm, Jarms *et al*. 2002) and covers the whole body, including the tentacles, at stage 12 (12.2 mm diameter, Jarms *et al*. 2002). Since this substance becomes toxic for the medusa when reacting on light (Jarms *et al*. 2002), the medusa must avoid exposure to day-light in the surface. Even if eggs are released close to dawn or dusk, the light attenuation (Fig. 8D) and sinking rate in the upper part of the water column ensure that the predation risk from visual predators will be low. Visual predators are probably the most important predators when light is available, due to their superior efficiency over tactile predators. Sørnes and Aksnes (2004) experimentally determined a critical lower irradiance level of 0.1 μmol photons m^{-2} s^{-1} where the ctenophore *Bolinopsis infundibulum* (a tactile predator) became more efficient than *Gobiusculus flavescens* (a small, shallow-living fish). If eggs of *P. periphylla* were released in twilight, with a subsurface solar irradiance of 10–20 μmol photons m^{-2} s^{-1}, and with the light attenuation we recorded for the visual spectrum (see results), this critical level would occur at 20–25 m. An egg released in the surface would reach that depth within 5–6 minutes. Pelagic fish like mackerel, herring and sprat, common along the Norwegian coast, hunt by vision, and are therefore limited in feeding by the light regime. Godö *et al*. (2004) surveyed mackerel (*Scomber scombrus*) schools in the Norwegian Sea, and found that their main distribution was between the surface and 40-m depth and never below 100-m depth. Cardinale *et al*. (2003) studied the vertical distribution and stomach fullness of herring (*Clupea harengus*) and sprat (*Sprattus sprattus*) in the Baltic Sea and found that both species had their main feeding periods in dawn and dusk, when they aggregated in the surface water. Since *P. periphylla* only remains in shallow water during night-time, where it probably spawns, predation pressure from day-hunting fish is therefore probably negligible. However, mesopelagic fish use a habitat with a low light regime and therefore with a depth that varies over the day. Rasmussen and Giske (1994) found that *Maurolicus muelleri* during daytime stayed in a depth where the light intensity was between 10^{-3} and 10^{-4} μmol photons m^{-2} s^{-1} but reached the surface in early night and descended to below 100 m before sunrise. Feeding was most intense during the night when staying in the surface water. Mesopelagic fish would thus be potential predators on eggs that are released in the surface during night-time. However, Lurefjord does not have a population of mesopelagic fish (Salvanes *et al*. 1995; Eiane *et al*. 1999), so eggs released by *P. periphylla* females in the surface during the night will therefore have a dark refuge from visual predators there. We can only speculate if the lack of observation of night-time surface occurrence in the two other fjords is an adaptation to avoid predation from mesopelagic fish on released eggs.

Sørnes *et al*. (2007) showed the striking difference in population structure between the three fjords, where Sognefjord diverged by being dominate by small (0.1–2 cm diameter) individuals to over 97% during all four research cruises, whereas the other two fjords had a population size structure where small individuals represented 20–60% of the population. They also showed that the abundance in Sognefjord was almost 10 times higher than in the other two fjords, then solely due to the high abundance of small individuals. Since our data came from 15 different cruises, where Lurefjord was always represented whereas Halsafjord was included in 5 and Sognefjord in 8 cruises, inter-annual variability might influence the results. However, Sørnes *et al*. (2007) included sampling from transects along the fjords during five cruises between October 2001 and October 2003. They did not find any statistical evidences for differences in population abundances between cruises, then including all sizes in the populations. Our abundance data over a considerably longer time span indicates significant variability (Fig. 5A) but the sampling program was not designed for a proper statistical evaluation of inter-annual variability.

Our results show that individuals of mature size were 4–5 times less abundant in Sognefjord compared to the other two fjords but with a much higher average size (Fig. 4). Since there is a strong exponential relationship between number of mature oocytes and female size (Fig. 6) an average mature female in Sognefjord carried 6–12 times more mature oocytes than an average mature female in the other two fjords (Fig. 8A). When mature oocytes are released, they will leave a signature in the gonad that is gradually resorbed, described as a follicle remnant (Tiemann and Jarms 2010). Such follicle remnants were found in our analyzed specimens of mature size, also in females without mature oocytes, as found in Lurefjord (Fig. 7), which is a strong evidences for a continuous reproduction over the whole mature life of the medusa.

Although female abundance was much lower in Sognefjord than in the other two fjords, the higher female fecundity caused the potential recruitment to become highest in this fjord (Fig. 7B). Part of the explanation could be the different habitat depths. Our quantitative results on vertical distribution of juveniles (<1 cm diameter, Fig. 9) show that small individuals had an abundance of 12 m^{-2} in Lurefjord, 20 m^{-2} in Halsafjord and 376 m^{-2} in Sognefjord, giving the numeric relationship 1:1.7:31.3 for the three fjords. Comparing these figures with the

theoretical recruitment rates (Fig. 7B), we get the corresponding numeric relationship of 1:2.1:2.5. Thus, the potential recruitment rate did not differ dramatically between the fjords, so the exceptionally high juvenile abundance in Sognefjord needs further explanation. The deeper distribution of juveniles in Sognefjord is an adaptation to the clearer basin water of Atlantic origin (Eiane *et al*. 1999), thereby providing shelter from visual predation in the same way as in the other two fjords. According to Sørnes *et al*. (2007), small (<4 cm diameter) individuals are not exposed to advective processes in any of the three fjords. Later estimates of the retention of small (<4 cm diameter) individuals have indicated even slightly lower retention in Sognefjord compared to Lurefjord (Dupont and Aksnes 2010). The population in Sognefjord must therefore differ by experiencing very low loss rate during early development. But since mature individuals were around 5 times less abundant in Sognefjord compared to the other two fjords (Fig. 4), there must be a much higher population loss during the later development to maturity, suggested by Sørnes *et al*. (2007) as a higher advective loss. This lower retention for big individuals in Sognefjord has been estimated through mathematical simulations to be 28% (Dupont and Aksnes 2010), which cannot account for the observed 5 times lower abundance we found (Fig. 4). Furthermore, since mature individuals are on average bigger (older) in Sognefjord (Fig. 4), part of the population appears to have a lower loss rate than in the other two fjords. An additional explanation for the situation in Sognefjord would be an advection-driven immigration of big, mature individuals that remain in the fjord. Detailed behavioural studies on vertical distribution of individuals like the ones been conducted in Lurefjord (Kaartvedt *et al*. 2011 and references therein) might help in explaining population differences between the three fjords. Learning how environmental factors govern the population dynamics of this globally distributed deep-water jellyfish will help to explain why some fjords are suitable habitats for mass occurrence of *P. periphylla*, and others are not.

CONCLUSION

Mating encounters of *P. periphylla* in Norwegian fjords are supposed to be strongly enhanced by the observed night-time surface aggregations we show for Lurefjord in the present study. Simulations show that fertilized eggs released in the surface within hours sink to a depth where light is insufficient for visual predators and where exchange of water with the open sea is low. The size structure within the fjord population is a key factor for female fecundity since the number of mature oocytes is exponentially related to the female size above the maturation size of 5–6 cm diameter. In a comparison of three fjords, we show that an average female in Sognefjord carried 6–12 times more mature oocytes than an average female in Halsafjord and Lurefjord. Although female abundance was around 5 times lower in Sognefjord than in the other two fjords, the potential recruitment rate as recruits m^{-2} $year^{-1}$ showed less variability, with a relative ratio of 1: 2.1: 2.5 (Lurefjord: Halsafjord: Sognefjord). A very high abundance of small (<1 cm diameter) juveniles in Sognefjord, 18–31 times higher than in the other two fjords, indicates that the deeper habitat in Sognefjord (up to 1300 m deep) compared to the other fjords (up to 440 and 530 m deep) was a superior habitat for eggs and the smallest juveniles.

ACKNOWLEDGEMENTS

Thanks are due to many students and scientists participating in different cruises over the years. We thank the University of Bergen for providing ship time and the crew on R/V Håkon Mosby for excellent technical support. We also thank the University of Bergen for working facilities at the Marine Biological Station and on-board R/V Håkon Mosby, and Umeå Marine Sciences Centre, Sweden and Institute of Zoology, University of Hamburg, Germany, for working facilities during preparation of the results. Comments from three anonymous referees helped in improving the manuscript and are thankfully acknowledged.

FUNDING

Norwegian Research Council (project nos. 108084/122; 146994/S40); EU-funded project EUROGEL (contract no EVK3-CT-32002-00074).

REFERENCES

Aksnes, D. L., Dupont, N., Staby, A., Fiksen, O., Kaartvedt, S. and Aure, J. (2009) Coastal water darkening and implications for mesopelagic regime shifts in Norwegian fjords. *Mar. Ecol. Prog. Ser.*, **387**, 39–49.

Bentlage, B., Cartwright, P., Yanagihara, A. A., Ames, C. L., Richards, G. S. and Collins, A. G. (2010) Evolution of box jellyfish (Cnidaria: Cubozoa), a group of highly toxic invertebrates. *Proc. Royal Society B: Biological Sci.*, **277**, 493–501.

Broch, H. (1913) Schyphomedusae from the Michael Sars North Atlantic deep-sea expedition 1910. *Report on the scientific results of the Michael Sars North Atlantic Deep-sea expedition 1910*, **3**, 1–20.

Brown, E. T. (1910) Coelenterata. V. Medusae. Reports of scientific results. National Antarctic Expedition 1901–1904. Natural history. *Zoology and Botany*, **5**, 62.

Bozman, A., Titelman, J., Kaartvedt, S., Eiane, K. and Aksnes, D. L. (2017) Jellyfish distribute vertically according to irradiance. *J. Plankton Res.*, **39**, 280–289.

Cardinale, M., Casini, M., Arrhenius, F. and Hakansson, N. (2003) Diel spatial distribution and feeding activity of herring (Clupea harengus) and sprat (Sprattus sprattus) in the Baltic Sea. *Aquat. Living Resour.*, **16**, 283–292.

Conklin, E. G. (1908) The habits and early development of *Linerges mercurius*. *Carnegie Inst. Wash. Publ.*, **103**, 153–170.

Dalpadado, P., Ellertsen, B., Melle, W. and Skjoldal, H. R. (1998) Summer distribution patterns and biomass estimates of macrozooplankton and micronekton in the Nordic seas. *Sarsia*, **83**, 103–116.

Dupont, N., Klevjer, T.A., Kaartvedt, S. and Aksnes, D.L. (2009) Diel vertical migration of the deep-water jellyfish Periphylla periphylla simulated as individual responses to absolute light intensity. *Limnology and Oceanography*, **54**, 1765–1775.

Eiane, K., Aksnes, D. L., Bagoien, E. and Kaartvedt, S. (1999) Fish or jellies - a question of visibility? *Limnol. Oceanogr.*, **44**, 1352–1357.

Fosså, J. H. (1992) Mass occurrence of *Periphylla periphylla* (Scyphozoa, Coronatae) in a Norwegian fjord. *Sarsia*, **77**, 237–251.

García-Rodríges, J., Lewis Ames, C., Marian, J. E. A. R. and Marques, A. C. (2018) Gonadal histology of box jellyfish (Cnidaria: Cubozoa) reveals variation between internal fertilizing species *Alatina alata* (Alatinidae) and *Copula sivickisi* (Tripedaliidae). *J. Morphol.*, **279**, 841–856.

Geoffroy, M., Berge, J., Majaneva, S., Johnsen, G., Langbehn, T. J., Cottier, F., Mogstad, A. A., Zolich, A. *et al.* (2018) Increase occurrence of the jellyfish *Periphylla periphylla* in the European high Arctic. *Polar Biol.*, **41**, 2615–2619.

Godo, O. R., Hjellvik, V., Iversen, S. A., Slotte, A., Tenningen, E. and Torkelsen, T. (2004) Behaviour of mackerel schools during summer feeding migration in the Norwegian Sea, as observed from fishing vessel sonars. *ICES J. Mar. Sci.*, **61**, 1093–1099.

Hargitt, C. W. and Hargitt, G. T. (1910) Studies in the development of Syphomedusae. *J. Morphol.*, **21**, 217–262.

Havnø, E. J. (1926) Periphylla hyacinthina. *Nature*, **50**, 286–287.

Holst, S. and Laakmann, S. (2014) Morphological and molecular discrimination of two closely related jellyfish species, *Cyanea capillata* and *C. lamarckii* (Cnidaria, Scyphozoa), from the Northeast Atlantic. *J. Plankton Res.*, **36**, 48–63.

Jarms, G., Båmstedt, U., Tiemann, H., Martinussen, M. B. and Fosså, J. H. (1999) The holopelagic life cycle of the deep-sea medusa *Periphylla periphylla* (Scyphozoa, Coronatae). *Sarsia*, **84**, 55–65.

Jarms, G., Tiemann, H. and Båmstedt, U. (2002) Development and biology of *Periphylla periphylla* (Scyphozoa: Coronatae) in a Norwegian fjord. *Mar. Biol.*, **141**, 647–657.

Kaartvedt, S., Titelman, J., Røstad, A. and Klevjer, T. A. (2011) Beyond the average: diverse individual migration patterns in a population of mesopelagic jellyfish. *Limnol. Oceanogr.*, **56**, 2189–2199.

Kaartvedt, S., Ugland, K. I., Klevjer, T. A., Røstad, A., Titelman, J. and Solberg, I. (2015) Social behaviour in mesopelagic jellyfish. *Sci. Rep.*, **5**, 1–8.

Kienberger, K., Riera-Buch, M., Schönemann, A. M., Bartsch, V., Halbaurer, R. and Prieto, L. (2018) First description oft he life cycle oft he jellyfish *Rhizostoma luteum* (Scyphozoa: Rhizostomeae). *PLoS One*, **13**(8), e0202093.

Kikinger, R. (1992) *Cotylorhiza tuberculata* (Cnidaria: Scyphozoa) – life history of a stationary population. *Mar. Ecol.*, **13**, 333–363.

Klevjer, T. A., Kaartvedt, S. and Båmstedt, U. (2009) In situ behaviour and acoustic properties of the deep living jellyfish *Periphylla periphylla*. *J. Plankton Res.*, **31**, 793–803.

Kramp, P. L. (1947) Medusae III. Trachylina and Scyphozoa, with zoogeographical remarks on all medusae of the northern Atlantic. *The Danish Ingolf-Expedition*, **5**, 1–92.

Kramp, P. L. (1968) The scyphomedusae collected by the Galathea expedition 1950–52. *Videnskabelige Meddelelser fra Dansk Naturhistoriska Förening*, **131**, 67–98.

Larson, R. J. (1986) Pelagic Scyphomedusae (Scyphozoa: Coronatae and Semaeostomeae) of the Southern Ocean. *Antarctic Res. Series*, **41**, 59–165.

Larson, R.J., Mills, C.E. and Harbison, G.R. (1991) Western Atlantic midwater hydrozoan and scyphozoan medusae: in situ studies using manned submersibles. *Hydrobiologia* **216/217,** 311–317.

Lewis, C. and Long, T. A. F. (2005) Courtshcip and reproduction in *Carybdea sivickisi* (Cnidaria: Cubozoa). *Mar. Biol.*, **147**, 477–483.

Lucas, C. H. and Reed, A. J. (2010) Gonad morphology and gametogenesis in the deep-sea jellyfish *Atolla wyvillei* and *Periphylla periphylla* (Scyphozoa: Coronatae) collected from cape Hatteras and the Gulf of Mexico. *J. Mar. Biol. Assoc. U. K.*, **90**, 1095–1104.

Mann, K. H. and Lazier, J. R. N. (1998) *Dynamics of marine ecosystems. Biological-physical interactions in the oceans*, Blackwell Science, Inc., Malden, USA.

Oakey, N. S. and Elliot, J. A. (1980) Dissipation in the mixed layer in Emerald Basin. In Nihoul, J. C. L. (ed.), *Marine turbulence*, Elsevier, Amsterdam, pp. 123–133.

Ohtsu, K., Kawahara, M., Ikeda, H. and Uye, S.-I. (2007) Experimental induction of gonadal maturation and spawning in the giant jellyfish *Nemopilema nomurai* (Scyphozoa: Rhizostomeae). *Mar. Biol.*, **152**, 667–676.

Osborn, D. A., Silver, M. W., Castro, C. G., Bros, S. M. and Chavez, F. P. (2007) The habitat of mesopelagic scyphomedusae in Monterey Bay, California. *Deep-Sea Research Part I-Oceanographic Research Papers*, **54**, 1241–1255.

Pages, F., White, M. G. and Rodhouse, P. G. (1996) Abundance of gelatinous carnivores in the nekton community of the Antarctic polar frontal zone in summer 1994. *Mar. Ecol. Prog. Ser.*, **141**, 139–147.

Rasmussen, O. I. and Giske, J. (1994) Life-history parameters and vertical distribution of *Maurolicus mulleri* in Masfjorden in summer. *Mar. Biol.*, **120**, 649–664.

Romeis, B.(1989) Mikroskopische Technik. Urban und Schwarzenberg, München pp. 697.

Rottini Sandrini, L. and Avian, M (1991) Rproduction of *Pelagia noctiluca* in the central and northern Adriatic Sea. *Hydrobiologia*, **216(**217), 197–202.

Salvanes, A. G. V., Aksnes, D., Fosså, J. H. and Giske, J. (1995) Simulated carrying capacities of fish in Norwegian fjords. *Fish. Oceanogr.*, **4**, 17–32.

Sneli, J. A. (1984) Masseopptreden av *Periphylla periphylla*. *Fauna*, **37**, 167.

Sørnes, T. A. and Aksnes, D. L. (2004) Predation efficiency in visual and tactile zooplanktivores. *Limnol. Oceanogr.*, **49**, 69–75.

Sørnes, T. A., Aksnes, D. L., Båmstedt, U. and Youngbluth, M. J. (2007) Causes for mass occurrences of the jellyfish *Periphylla periphylla*: a hypothesis that involves optically conditioned retention. *J. Plankton Res.*, **29**, 157–167.

Stiasny, G. (1934) Scyphomedusae. *Discovery Reports*, **8**, 329–396.

Tiemann, H. and Jarms, G. (2010) Organ-like gonads, complex oocyte formation, and long-term spawning in *Periphylla periphylla* (Cnidaria, Scyphozoa, Coronatae). *Mar. Biol.*, **157**, 527–535.

Tiemann, H., Sötje, I., Johnston, B. D., Flood, P. R. and Båmstedt, U. (2009) Documentation of potential courtship-behaviour in *Periphylla periphylla* (Cnidaria: Scyphozoa). *J. Mar. Biol. Assoc. U. K.*, **89**, 63–66.

Tiller, R. G., Borgersen, A. L., Knutsen, O., Bailey, J., Bjelland, H. V., Mork, J., Eisenhauer, L. and Liu, Y. J. (2017) Coming soon to a fjord near you: future jellyfish scenarios in a changing climate. *Coast. Manag.*, **45**, 1–23.

Tiller, R. G., Mork, J., Liu, Y. J., Borgersen, A. L. and Richards, R. (2015) To adapt or not adapt: assessing the adaptive capacity of artisanal fishers in the Trondheimsfjord (Norway) to jellyfish (*Periphylla periphylla*) bloom and purse seiners. *Marine and Coastal Fisheries*, **7**, 260–273.

Toshino, S., Miyake, H., Srinui, K., Luangoon, N., Muthuwan, V., Sawatpeera, S., Honda, S. and Shibata, H. (2017) Development of *Tripedalia bineata* Moore, 1988 (Cubozoa: Carybdeida: Tripedaliidae) collected from the eastern gulf of Thailand with implications for the phylogeny of the Cubozoa. *Hydrobiologia*, **792**, 37–51.

Turner, J. P. and Lucas, C. H. (2010) Population structure, reproduction and morphological characteristics of *Periphylla periphylla* in the Iceland Basin. *Mar. Biol.*

Uchida, T. (1926) The anatomy and development of a Rhizostome medusa, *Mastigias papua* L. Agassiz, with observations on the phylogeny of Rhizostomae. *J. Faculty of Sci. Imperial University of Tokyo, Section IV Zoology*, **1**, 45–95.

Ueno, S. and Mitsutani, A. (1994) Small-scale swarm of a hydrozoan medusa *Lirope tetraphylla* in Hiroshima Bay, the Inland Sea of Japan. *Bull. Plankton Soc. Japan*, **41**, 165–166.

Werner, B. (1973) Spermatozeugmen und Paarungsverhalten bei *Tripedalia cystophora* (Cubomedusae). *Mar. Biol.*, **18**, 212–217.

Widersten, B. (1965) Genital organs and fertilization in some Syphozoa. *Zoologiska Bidrag Fran Uppsala*, **37**, 45–58.

Youngbluth, M. J. and Båmstedt, U. (2001) Distribution, abundance, behavior and metabolism of *Periphylla periphylla*, a mesopelagic coronate medusa in a Norwegian fjord. *Hydrobiologia*, **451**, 321–333.